533
10/3/84

(1)

I-17274

DR 0438-3

SANDIA REPORT SAND84—0956 • Unlimited Release • UC—66c
Printed August 1984

Numerical Results for the Solution of the Graetz Problem for a Bingham Plastic in Laminar Tube Flow with Constant Wall Temperature

SAND--84-0956

DE85 001883

B. F. Blackwell

Prepared by
Sandia National Laboratories
Albuquerque, New Mexico 87185 and Livermore, California 94550
for the United States Department of Energy
under Contract DE-AC04-76DP00789

DISCLAIMER

Issued by Sandia National Laboratories, operated for the United States Department of Energy by Sandia Corporation.

Printed in the United States of America
Available from
National Technical Information Service
U.S. Department of Commerce
5285 Port Royal Road
Springfield, VA 22161

NTIS price codes
Printed copy: A02
Microfiche copy: A01

SAND84-0956

Numerical Results for the Solution of the Graetz Problem for a Bingham Plastic in Laminar Tube Flow with Constant Wall Temperature

B. F. Blackwell
Sandia National Laboratories*
Centrifuge, Climatic and Radiant Heat
Division 7531

ABSTRACT

The Graetz problem of developing temperature profile in a tube for a fully developed laminar velocity profile has been numerically solved for a Bingham plastic. Constant properties were assumed and viscous dissipation was ignored. Results are presented for local Nusselt number, average Nusselt number, and bulk fluid temperature each as a function of axial distance from the tube inlet. The laminar Newtonian fluid is a special case of the Bingham plastic; the results presented in this article for this case appear to be more accurate than those available in the literature.

*Sandia National Laboratories is a U.S. Department of Energy facility. This work was supported by the Department of Energy under contract DE-AC0476DP00789.

TABLE OF CONTENTS

LIST OF FIGURES

NOMENCLATURE

c	τ_y/τ_w, ratio of yield stress to wall shear stress
C_p	specific heat at constant pressure
C_n	constant in series solution
D	pipe diameter
G_n	constant, see Eq. (12)
h_x	local convective heat transfer coefficient, $h_x = \dot{q}''/(t_b - t_o)$
k	thermal conductivity
Nu_x	$= h_x D/k$, local Nusselt number
Nu_m	average of Nu_x between entrance and axial location x
$\dot{q}''(x)$	wall heat flux
Pe	$= \bar{u}D/\alpha$, Peclet number
r	radial coordinate
r_o	pipe radius
r^+	$= r/r_o$, dimensionless radius
$R_n(r^+)$	eigenfunction
$t(x,r)$	temperature
t_b	bulk or mixing cup temperature
t_e	uniform entrance temperature
t_o	uniform wall temperature
$u(r)$	axial velocity
u_{max}	maximum axial velocity
$\bar{u}$	average axial velocity
u^+	$= u/\bar{u}$
x	axial coordinate
x^+	$= \dfrac{x/r_o}{Pe}$, dimensionless axial coordinate

GREEK

α = $k/\rho C_p$, thermal diffusivity

η Bingham viscosity

θ = $\dfrac{t_o - t(x,r)}{t_o - t_e}$, dimensionless temperature

θ_b = $\dfrac{t_o - t_b}{t_o - t_e}$, dimensionless bulk fluid temperature, see Eq. (13)

λ eigenvalue

ρ density

τ local shear stress

τ_w wall shear stress

τ_y yield shear stress

Numerical Results for the Solution of the Graetz Problem for a Bingham Plastic in Laminar Tube Flow with Constant Wall Temperature

INTRODUCTION

Many fluids exhibit a yield stress, a stress which must be exceeded before the fluid will flow. Bird, et. al. [1] presented an extensive tabulation of materials with yield stresses; some common examples are drilling mud, sewage sludge, grease, paint, and thorium dioxide/methanol. If the local shear stress does not exceed the yield stress, these fluids will not support a velocity gradient. In pipe flow geometries, it is possible that the fluid region near the centerline (low shear stress, $\tau<\tau_y$) may move as a solid (plug flow) while the fluid near the wall (high shear stress, $\tau>\tau_y$) supports a velocity gradient. Figure 1 presents representative laminar velocity profiles for Bingham plastics that exhibit a plug flow region.

This article was motivated by the desire to understand the heat transfer behavior of aqueous foams being used as a drilling fluid in high temperature petroleum and geothermal formations. In some applications, aqueous foams offer several advantages over conventional drilling fluids: 1) bottom hole pressure is reduced because aqueous foams have a much lower density than conventional drilling muds, 2) relatively little fall back of cuttings when circulation stops, and 3) low loss of circulation in porous formations. Additional details on the thermal behavior of aqueous foams circulating in geothermal wellbores are presented in Blackwell and Ortega [2]. This report is an extension of the work of Wissler and Schechter [3] concerning the heat transfer behavior of Bingham plastics in developing tube flow. Slip at the wall has been ignored in this analysis.

ANALYSIS

The constitutive equation for a Bingham plastic in pipe flow is of the form [1,3,4]

$$\frac{du}{dr} = 0 \quad \text{for } \tau \leq \tau_y$$

$$-\frac{du}{dr} = \frac{1}{\eta}(\tau - \tau_y) \quad \text{for } \tau \geq \tau_y \tag{1}$$

where u is the axial velocity component, r is the radial coordinate, τ is the local shear stress, τ_y is the yield stress, and η is the Bingham viscosity. For constant properties, the fully developed velocity profile has been shown to be [1,3,4]

$$u = \frac{\tau_w r_o}{2\eta}\left[1 - \left(\frac{r}{r_o}\right)^2 - 2c\left(1 - \frac{r}{r_o}\right)\right] \qquad c \leq \frac{r}{r_o} \leq 1 \tag{2}$$

$$u = u_{max}\,, \qquad 0 \leq \frac{r}{r_o} \leq c$$

where τ_w is the wall shear stress, r_o is the pipe radius, and $c=\tau_y/\tau_w$. The maximum velocity u_{max} and the average velocity can be expressed as

$$u_{max} = \frac{\tau_w r_o}{2\eta}(1-c)^2 \tag{3}$$

$$\bar{u} = \frac{\tau_w r_o}{4\eta}\left(1 - \frac{4}{3}c + \frac{c^4}{3}\right) \tag{4}$$

The dimensionless form of Eq.(4) is presented in Fig. 1. Note that c=1 corresponds to plug flow ($u=u_{max}$) while c=0 corresponds to laminar Newtonian flow.

If axial conduction is neglected (Pe>100) and viscous dissipation ignored, the steady flow constant property form of the energy equation and its boundary conditions can be written as

$$\rho C_p u(r)\frac{\partial t}{\partial x} = k\frac{1}{r}\frac{\partial}{\partial r}\left(r\frac{\partial t}{\partial r}\right)\,, \quad t(o,r)=t_e,\; t(x,r_o)=t_o, \tag{5}$$

$$\frac{\partial t}{\partial r}(x,o) = 0$$

This analysis is restricted to Prandtl number>1 but still sufficiently small that viscous dissipation is not important. The following dimensionless variables will be useful:

$$\theta = \frac{t_o - t(x,r)}{t_o - t_e} \ , \ r^+ = \frac{r}{r_o} \ , \ u^+ = \frac{u}{\bar{u}} \ , \ x^+ = \frac{x/r_o}{Pe}, \ Pe = \frac{\bar{u}D}{\alpha} \quad (6)$$

where t_o is the wall temperature, t_e, is the uniform inlet fluid temperature, α is the thermal diffusivity, and Pe is the dimensionless Peclet number. For uniform wall temperature t_o and inlet temperature t_e, the dimensionless energy equation is

$$\frac{u^+}{2}\frac{\partial\theta}{\partial x^+} = \frac{1}{r^+}\frac{\partial}{\partial r^+}\left(r^+\frac{\partial\theta}{\partial r^+}\right) \ , \ \theta(o,r^+)=1, \ \theta(x^+,1)=o, \ \frac{\partial\theta(x^+,o)}{\partial r^+} = 0 \quad (7)$$

with the dimensionless velocity profile being given by

$$u^+ = \frac{2[1-r^{+2}-2c(1-r^+)]}{1-\frac{4}{3}c+\frac{c^4}{3}} \qquad c \le r^+ \le 1$$

$$= \frac{2(1-c)^2}{1-\frac{4}{3}c+\frac{c^4}{3}} \qquad o \le r^+ \le c \quad (8)$$

The classical separation of variables solution to Eq. (7) leads to

$$\theta(x^+,r^+) = \sum_{n=0}^{\infty} C_n R_n(r^+)\exp(-\lambda_n^2 x^+) \quad (9)$$

where C_n is a constant to be determined from the boundary conditions and $R_n(r^+)$ and λ_n are eigenfunctions and eigenvalues respectively that are determined from the solution of

$$\frac{d}{dr^+}\left(r^+\frac{dR_n}{dr^+}\right) + \lambda_n^2\frac{u^+}{2}r^+R_n = 0 \qquad R_n(1)=0 \ , \ \frac{dR_n(0)}{dr^+}=0 \quad (10)$$

From the orthogonality condition,

$$C_n = \frac{\int_0^1 \frac{u^+}{2} r^+ R_n dr^+}{\int_0^1 \frac{u^+}{2} r^+ R_n^2 dr^+} = \frac{\frac{-2}{\lambda_n^2} \frac{dR_n(1)}{dr^+}}{\int_0^1 u^+ r^+ R_n^2 dr^+} \tag{11}$$

A more convenient constant G_n will be defined as

$$G_n = -\frac{C_n}{2} \frac{dR_n(1)}{dr^+} = \frac{[dR_n(1)/dr^+]^2/2}{\lambda_n^2 \int_0^1 \frac{u^+}{2} r^+ R_n^2 dr^+} \tag{12}$$

From Eq. (9), several useful heat transfer parameters can be developed. The dimensionless bulk fluid temperature is

$$\theta_b(x^+) = \frac{t_o - t_b}{t_o - t_e} = 2 \int_0^1 u^+ \theta r^+ dr^+ = 8 \sum_{n=0}^{\infty} \frac{G_n}{\lambda_n^2} \exp(-\lambda_n^2 x^+) \tag{13}$$

where t_b is the bulk fluid or mixing cup temperature. Defining the local heat transfer coefficient in terms of the local temperature difference $(t_b - t_o)$, the local Nusselt number becomes

$$Nu_x = \frac{h_x D}{k} = \frac{-2}{\theta_b} \frac{\partial \theta(x,1)}{\partial r^+} = \frac{4}{\theta_b} \sum_{n=0}^{\infty} G_n \exp(-\lambda_n^2 x^+) \tag{14}$$

The average Nu between the entrance and any arbitrary x^+ is given quite simply by

$$Nu_m(x^+) = \frac{1}{x^+} \int_o^{x^+} Nu_x dx^+ = \frac{1}{2x^+} \ln(1/\theta_b) \tag{15}$$

Eq.(10) is the classical Sturm-Liouville problem. A closed form analytical solution exists for plug flow (c=1, see Burmeister [5] for a discussion), Sellars, Tribus, and Klein [6] developed an approximate solution for laminar Newtonian flow (c=0), and Wissler and Schechter [3] numerically determined the first seven eigenvalues and eigenfunctions for c=0.0, 0.25, 0.5, 0.75, and 1.0. Additional works are referenced in [1]. The number of eigenvalues and eigenfunctions reported by Wissler and Schechter [3] were found to be inadequate for small values of x^+ and the calculations were extended to include the first 60 eigenvalues for c=0.0, 0.2, 0.4, 0.6, 0.8, 1.0.

The general Sturm-Liouville problem can be written as

$$\frac{d}{dx}\left(p(x)\frac{d}{dx}\psi(x)\right) + (q(x) + \lambda r(x))\psi(x) = 0 \qquad a \le x \le b \tag{16}$$

with boundary conditions of the form

$$\begin{aligned} A_1\psi(a) + A_2 p(a)\frac{d}{dx}\psi(a) &= 0 \\ B_1\psi(b) + B_2 p(b)\frac{d}{dx}\psi(b) &= 0 \end{aligned} \tag{17}$$

where p(x), q(x), and r(x) are arbitrary functions and $\psi(x)$ is the eigenfunction. The numerical results presented in this article were produced by the SLEIGN code, described by Bailey [7]. This code internally transforms the independent variable x onto the interval (-1,1). Next, the second order differential equation given by Eq. (16) is replaced (within the code) by an equivalent system of two first order equations for the new dependent variables $\rho(x)$ and $\phi(x)$ defined by

$$\begin{aligned} \psi(x) &= \rho(x)\sin\phi(x) \\ p(x)\psi'(x) &= z\rho(x)\cos\phi(x) \end{aligned} \tag{18}$$

where z is a scaling factor determined by the code. If z=1, this is known as the Prufer transformation [7]. The eigenvalue λ is then determined by numerically integrating the transformed version of Eq. (16) from both boundaries toward the interior of the internal (a,b) with an assumed λ. The integration is terminated at an interior point x=M and the solution from the left

$\psi_L(M;\lambda)$ is compared with the solution from the right $\psi_R(M;\lambda)$. During both the "left" and "right" integration process, the correct boundary conditions are always used. The code automatically chooses the match point x=M, picks an initial guess for λ and adjusts λ until $\psi_L=\psi_R$ within a user specified tolerance. The code has been extensively tested and additional details can be found in Bailey [7].

RESULTS

Table 1 presents numerical results for the local Nusselt number (Nu_x), average Nusselt number Nu_m, and bulk fluid temperature as a function of the dimensionless entry length x^+. All calculations were performed on a CDC Cyber 170/Model 855 computer using single precision arithmetic (nominally 14 1/2 digits). The series for Nu_x converges more slowly than that for θ_b. A relative convergence criteria of 10^{-6} on the last term (normalized by the partial sum) was used. Sixty eigenvalues were adequate for convergence for all values of x^+ except 0.0001; for this x^+, the relative error was typically less than $7x10^{-5}$ for all values of c. The numerical results for c=1.0 were compared with the analytical solution; for this case, the eigenvalues are the roots of $J_o(\lambda_n/\sqrt{2}) = 0$ and the eigenfunctions are $R_n(r^+) = J_o(\lambda_n/\sqrt{2}\ r^+)$. The results from SLEIGN were identical to the analytical solution for the number of significant digits printed, except for $x^+ = 0.0001$. For example, the analytical result was $Nu_x = 81.352$ while the numerical result was 81.365. The c=1 (plug flow) results were also compared with those presented in Burmeister [5]; exact agreement was obtained for large x^+ but it appears that the results of [4] are not accurate at small x^+.

Sellars, Tribus, and Klein [6] developed an approximate solution for c=0 (laminar Newtonian flow) and their results for Nu_x, Nu_m, and θ_b are tabulated in Kays and Crawford [8] and Burmeister [9]. Again, these results do not appear to be accurate at small x^+.

The results of Table 1 are also presented graphically in Figures 2-4. For c near zero, Nu and the bulk fluid temperature are not very sensitive to c; for c near unity, the computed results are much more sensitive to c. These results stem from the dependence of the velocity profile on c (see Fig. 1).

CONCLUSIONS

The numerical solution of the Graetz problem of the development of the thermal boundary layer within a tube for laminar fully developed velocity profile under a constant wall temperature boundary condition was presented for a Bingham plastic. Local Nusselt number, average Nusselt number and bulk fluid temperature were presented as a function of dimensionless distance from the inlet. The results for plug flow agree with the analytical solution, and the laminar Newtonian flow (c=0) results of this work appear to be more accurate than those available in the literature.

Table 1 Heat Transfer Results for Developing Flow of Bingham Plastic in a Tube with Constant Wall Temperature

c=1.0 (plug flow)

x^+	Nu_x	Nu_m	θ_b
.0001	81.352	161.146	.9682847
.0002	58.008	114.413	.9552662
.0004	41.502	81.375	.9369734
.0010	26.876	52.074	.9010919
.0020	19.531	37.322	.8613197
.0040	14.372	26.914	.8062926
.0100	9.844	17.731	.7014360
.0200	7.744	13.174	.5904024
.0400	6.437	10.063	.4470782
.1000	5.817	7.620	.2178524
.2000	5.783	6.705	.0684313
.4000	5.783	6.244	.0067703
1.0000	5.783	5.968	.0000066
2.0000	5.783	5.875	.0000000
4.0000	5.783	5.829	.0000000
10.0000	5.783	5.802	.0000000

c=0.8

x^+	Nu_x	Nu_m	θ_b
.0001	39.913	60.569	.9879594
.0002	31.453	47.802	.9810610
.0004	24.774	37.701	.9702898
.0010	18.079	27.529	.9464307
.0020	14.271	21.704	.9168451
.0040	11.299	17.129	.8719433
.0100	8.366	12.569	.7777295
.0200	6.777	10.003	.6702263
.0400	5.703	8.069	.5243750
.1000	5.111	6.401	.2779934
.2000	5.066	5.738	.1007254
.4000	5.066	5.402	.0132775
1.0000	5.066	5.200	.0000304
2.0000	5.066	5.133	.0000000
4.0000	5.066	5.099	.0000000
10.0000	5.066	5.079	.0000000

c=0.6

x^+	Nu_x	Nu_m	θ_b
.0001	33.304	50.486	.9899536
.0002	26.265	39.866	.9841801
.0004	20.706	31.462	.9751443
.0010	15.135	22.998	.9550453
.0020	11.972	18.153	.9299621
.0040	9.520	14.353	.8915229
.0100	7.149	10.591	.8091051
.0200	5.892	8.503	.7116963

Table 1 Heat Transfer Results for Developing Flow of Bingham Plastic in a Tube with Constant Wall Temperature (Cont)

c=0.6

x^+	Nu_x	Nu_m	θ_b
.0400	5.038	6.943	.5738254
.1000	4.539	5.593	.3267612
.2000	4.494	5.048	.1327436
.4000	4.493	4.771	.0220013
1.0000	4.493	4.604	.0001002
2.0000	4.493	4.549	.0000000
4.0000	4.493	4.521	.0000000
10.0000	4.493	4.504	.0000000

c=0.4

x^+	Nu_x	Nu_m	θ_b
.0001	30.513	46.252	.9907923
.0002	24.065	36.524	.9854966
.0004	18.970	28.825	.9772039
.0010	13.860	21.068	.9587394
.0020	10.956	16.625	.9356627
.0040	8.703	13.139	.9002269
.0100	6.520	9.684	.8239285
.0200	5.364	7.764	.7330460
.0400	4.585	6.332	.6025852
.1000	4.126	5.094	.3610479
.2000	4.082	4.593	.1592788
.4000	4.081	4.337	.0311343
1.0000	4.081	4.183	.0002326
2.0000	4.081	4.132	.0000001
4.0000	4.081	4.106	.0000000
10.0000	4.081	4.091	.0000000

c=0.2

x^+	Nu_x	Nu_m	θ_b
.0001	29.061	44.053	.9912281
.0002	22.921	34.788	.9861812
.0004	18.066	27.454	.9782760
.0010	13.196	20.064	.9606662
.0020	10.426	15.830	.9386436
.0040	8.274	12.505	.9047981
.0100	6.186	9.208	.8318034
.0200	5.075	7.372	.7446142
.0400	4.319	5.999	.6188482
.1000	3.861	4.803	.3826712
.2000	3.814	4.314	.1780752
.4000	3.813	4.063	.0387508
1.0000	3.813	3.913	.0003994
2.0000	3.813	3.863	.0000002
4.0000	3.813	3.838	.0000000
10.0000	3.813	3.823	.0000000

Table 1 Heat Transfer Results for Developing Flow of Bingham Plastic in a Tube with Constant Wall Temperature (Cont)

c=0.0 (Laminar Newtonian)

x^+	Nu_x	Nu_m	θ_b
.0001	28.244	42.814	.9914737
.0002	22.278	33.810	.9865668
.0004	17.559	26.683	.9788795
.0010	12.824	19.501	.9617496
.0020	10.130	15.384	.9403183
.0040	8.036	12.152	.9073635
.0100	6.002	8.943	.8362189
.0200	4.916	7.155	.7511056
.0400	4.172	5.815	.6280276
.1000	3.710	4.641	.3952988
.2000	3.658	4.156	.1897101
.4000	3.657	3.906	.0439350
1.0000	3.657	3.757	.0005458
2.0000	3.657	3.707	.0000004
4.0000	3.657	3.682	.0000000
10.0000	3.657	3.667	.0000000

REFERENCES

1. R.B. Bird, G.C. Dai, and B.J. Yarusso, The Rheology and Flow of Viscoplastic Materials, Reviews in Chemical Engineering, Vol. 1, No. 1, 1982, pp 1-70.

2. B.F. Blackwell and A. Ortega, A Quasi-Steady Model for Predicting Temperature of Aqueous Foams Circulating in Geothermal Wellbores, Proceedings ASME/JSME Thermal Engineering Joint Conference, Vol II, pp 101-111, 1983.

3. E.H. Wissler and R.S. Schechter, The Graetz-Nusselt Problem (with Extension) for a Bingham Plastic, Chemical Engineering Progress Symposium Series No. 29, Vol 55, pp 203-208 (1959).

4. R.B. Bird, W.E. Stewart, and E.N. Lightfoot, Transport Phenomena, Wiley, New York, 1960.

5. L.C. Burmeister, Convective Heat Transfer, John Wiley, New York, 1983.

6. J.R. Sellars, M. Tribus, and J.S. Klein, Heat Transfer to Laminar Flow in a Round Tube or Flat Conduit-The Graetz Problem Extended, Transactions ASME, Vol 78, pp 441-448, Feb. 1956.

7. P.B. Bailey, SLEIGN An Eigenvalue-Eigenfunction Code for Sturm-Liouville Problems, Sandia National Laboratories, SAND77-2044, March 1978.

8. W.M. Kays and M.E. Crawford, Convective Heat and Mass Transfer, 2nd Ed., McGraw-Hill, New York, 1980.

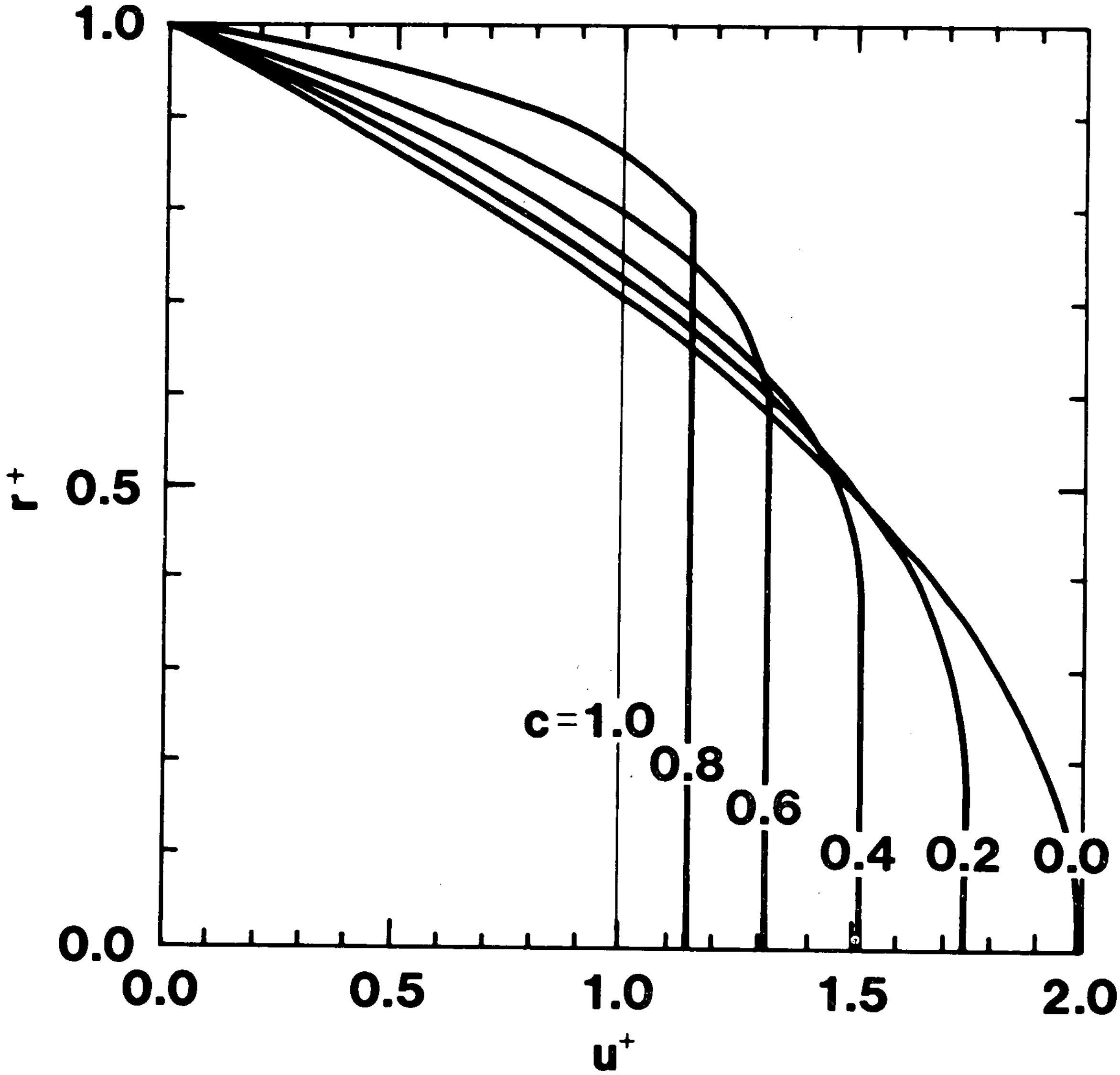

Figure 1 Dimensionless Velocity Profile for Fully Developed Flow of a Bingham Plastic in Circular Tube ($c=\tau y/\tau w$)

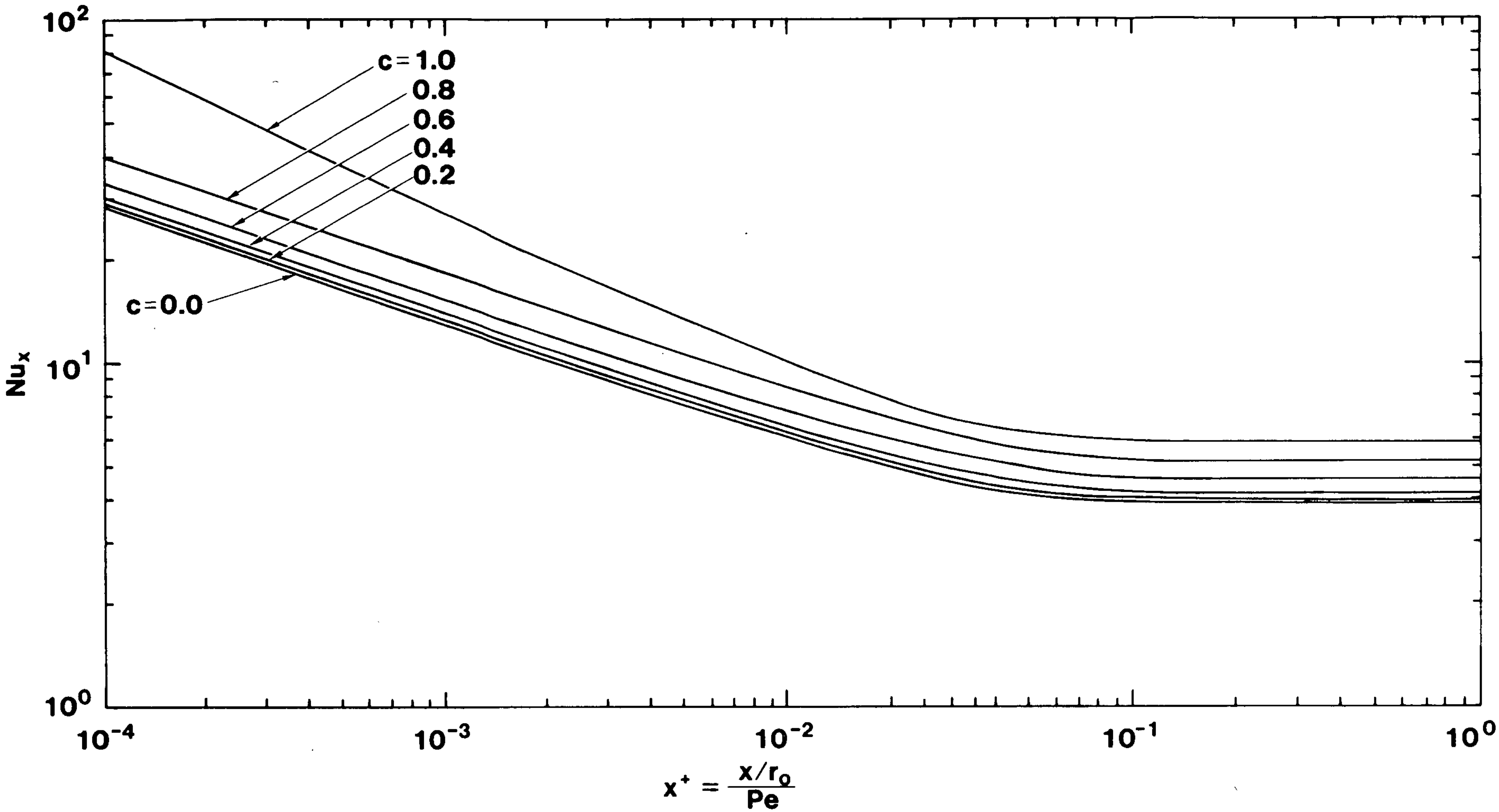

Figure 2 Variation of Local Nusselt No (Nu_x) with Dimensionless Axial Distance $\frac{(x/r_o)}{Pe}$ for c=0.0, 0.2, 0.4, 0.6, 0.8, and 1.0.

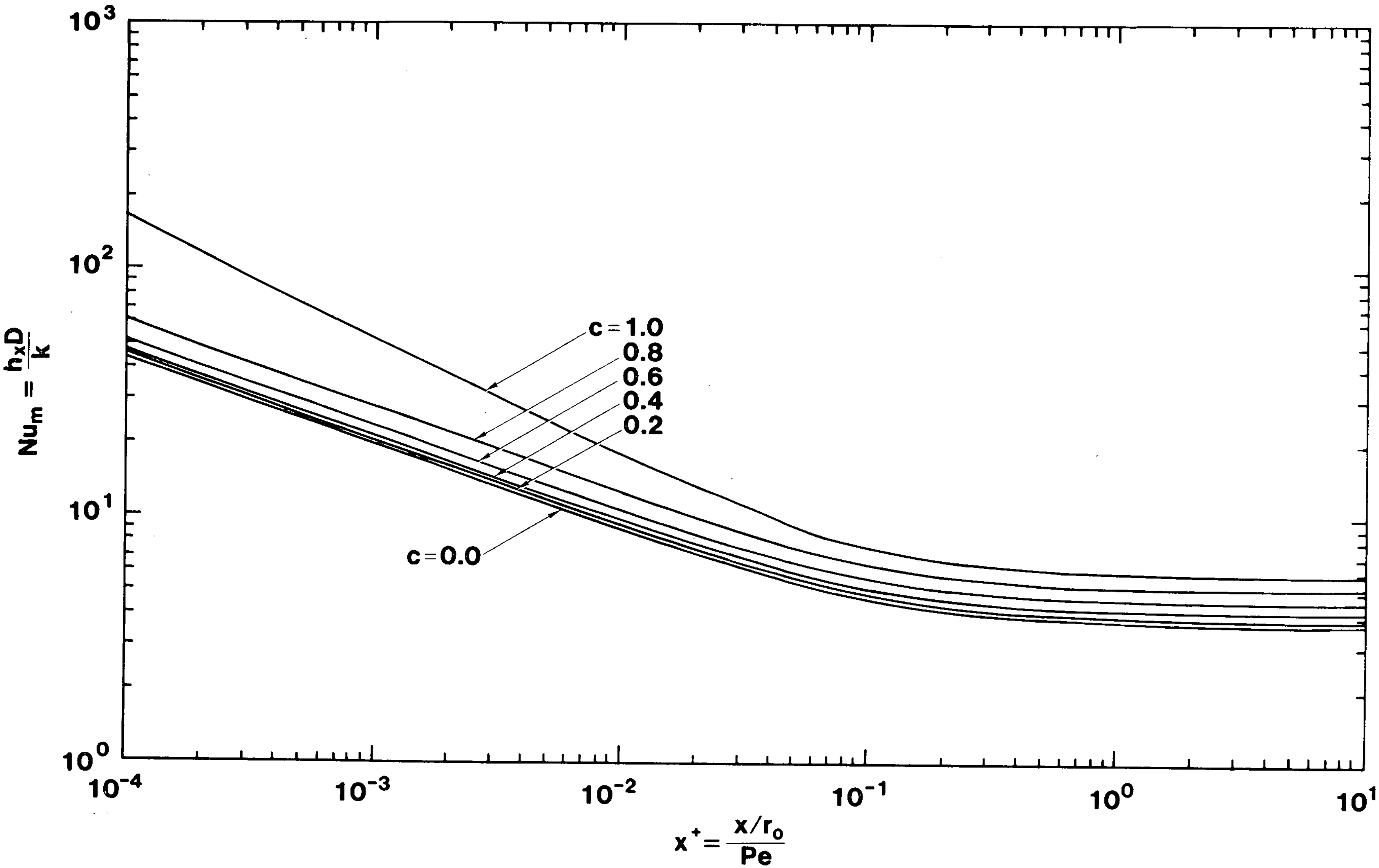

Figure 3 Variation of Mean Nusselt No (Nu_m) with Dimensionless Axial Distance $\frac{(x/r_o)}{Pe}$ for c=0.0, 0.2, 0.4, 0.6, 0.8, and 1.0.

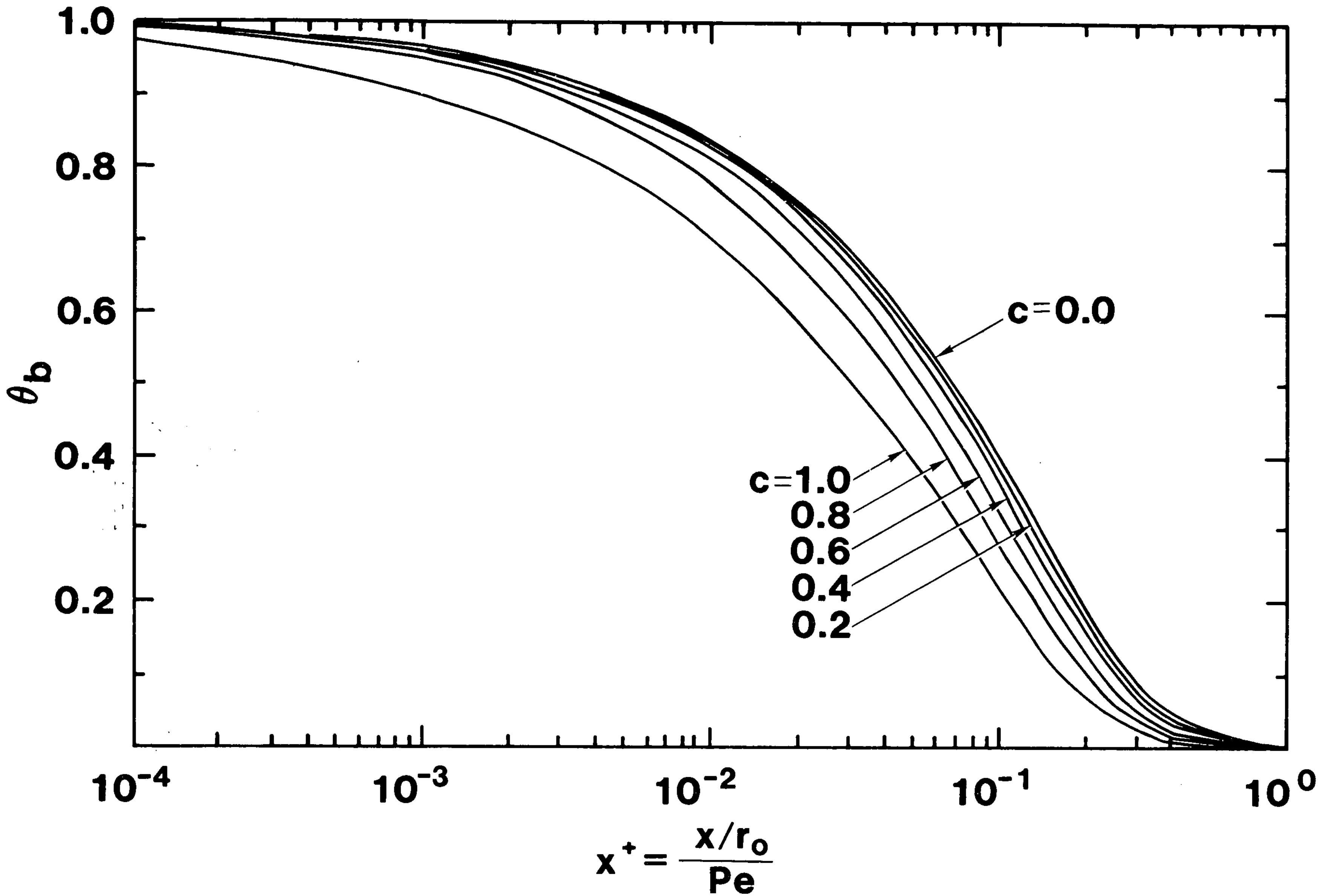

Figure 4 Variation of Dimensionless Bulk Fluid Temperature (θ_b) with Dimensionless Axial Distance $\frac{(x/r_o)}{Pe}$ for c=0.0, 0.2, 0.4, 0.6, 0.8, and 1.0.

Distribution:

TID-4500-R-66-UC-66c (507)

Advanced Drilling Corp.
2060 Plymouth St.
Mountain View, CA 94043
Attn: W. Littmann

Tom Anderson
17726 S.W.
Overlook Inn,
Lake Oswego, OR 97034

Ed Bingman
Shell Oil Company
Two Shell Plaza
P.O. Box 2099
Houston, TX 77001

Christensen, Inc.
Diamond Technology Center
2532 South 3270 West
Salt Lake City, UT 84119
Attn: Jim Carroll

Larry Diamond
Dyna-Drill
P.O. Box C-19576
Irvine, CA 92713

John E. Fontenot
NL Petroleum Services
P.O. Box 60087
Houston, TX 77205

Dr. Melvin Friedman
Professor of Geology
Center for Tectonophysics
and Dept. of Geology
Texas A&M University
College Station, TX 77843

Galveston-Houston Company
5229 Winfield
P.O. Box 2207
Houston, TX 77001
Attn: J. K. Heilhecker

James W. Lanford
Security Division
Dresser Industries, Inc.
P.O. Box 24647
Dallas, TX 75224

B. J. Livesay
2616 Angell Ave.
San Diego, CA 92122

Harvey E. Mallory
P.O. Box 54696
Tulsa, OK 74155

Ed Martin
Superior Oil
Eastern Division
P.O. Box 51108 OCS
Lafayette, LA 70505

Meridian Corporation
5113 Leesburg Pike
Suite 700
Falls Church, VA 22041
Attn: Deepak Kenkeremath

Maurer Engineering Inc.
2916 West T.C. Jester
Houston, TX 77018
Attn: W. C. Maurer

Gene Polk
NL Baroid
6400 Uptown Blvd. N.E. 365W
Albuquerque, NM 87110

Del E. Pyle
Union Geothermal Division
Union Oil Co. of California
Union Oil Center
Los Angeles, CA 90017

John C. Rowley
Los Alamos National Labs.
Mail Stop 570
Los Alamos, NM 87545

Prof. Barry Raleigh
Lamont Doherty Geological
Observatory of Columbia
University
Palisades, NY 10964

William D. Rumbaugh
Research and Development
Otis
P.O. Box 34380
Dallas, TX 75234

Ed Schmidt
400 East 57th St.
New York, NY 10022

Dwight Smith
Halliburton
Drawer 1431
Duncan, OK 73533

N.L. Sperry Sun
P.O. Box 69
Sugar Land, TX 77479
Attn: Dr. S. G. Varnado

Tom Warren
Phillips Petroleum Company
Geothermal Operations
655 East 4500 South
Salt Lake City, UT 84107

U.S. Department of Energy (8)
Office of Energy Research
Washington, DC 20545
Attn: George Y. Jordy ER 31 (7)
Robert E. Rader ER 32

U.S. Department of Energy (3)
Geothermal Hydropower
Technologies Division
Forrestal Bldg., C.E. 324
1000 Independence Ave. S.W.
Washington, DC 20585
Attn: J. Bresee
R. Toms
D. Allen

U.S. Department of Energy
Office of Basic Energy Sciences
Mail Stop J309
Washington, DC 20585
Attn: George Kolstad

W. K. Technology
9777 Harwin Dr.
Suite 408
Houston, TX 77036
Attn: Frank O'Brien

W. P. Grace, DOE/ALO
Nuclear & Geosciences
Division

1512 J. C. Cummings
attn: L. A. Mondy
1513 D. W. Larson
attn: S. K. Griffiths
1813 A. M. Kraynik
1813 P. B. Rand
1824 W. D. Drotning
3141 L. J. Erickson (5)
3151 W. L. Garner (3)
6000 E. H. Beckner
6200 V. L. Dugan
6240 R. K. Traeger
6241 J. R. Kelsey
6241 L. E. Duda (20)
6246 B. Granoff
6247 P. J. Hommert
6250 B. W. Marshall
6252 H. M. Dodd
6256 D. Engi
7530 T. B. Lane
7531 B. F. Blackwell (10)
7537 N. R. Keltner
8214 M. A. Pound